

# Instrumentation and system identification of a typical school building in Istanbul

Pelin Gundes Bakir\*

*Department of Civil Engineering, Istanbul Technical University, Pembegulsok,  
Pelin apt. No:20 D:5 Suadiye, Istanbul, Turkey*

*(Received February 1, 2011, Revised April 4, 2012, Accepted May 31, 2012)*

**Abstract.** This study presents the findings of the structural health monitoring and the real time system identification of one of the first large scale building instrumentations in Turkey for earthquake safety. Within this context, a thorough review of steps in the instrumentation, monitoring is presented and seismic performance evaluation of structures using both nonlinear pushover and nonlinear dynamic time history analysis is carried out. The sensor locations are determined using the optimal sensor placement techniques used in NASA for on orbit modal identification of large space structures. System identification is carried out via the stochastic subspace technique. The results of the study show that under ambient vibrations, stocky buildings can be substantially stiffer than what is predicted by the finite element models due to the presence of a large number of partitioning walls. However, in a severe earthquake, it will not be safe to rely on this resistance due to the fact that once the partitioning walls crack, the bare frame contributes to the lateral stiffness of the building alone. Consequently, the periods obtained from system identification will be closer to those obtained from the FE analysis. A technique to control the validity of the proportional damping assumption is employed that checks the presence of phase difference in displacements of different stories obtained from band pass filtered records and it is confirmed that the "proportional damping assumption" is valid for this structure. Two different techniques are implemented for identifying the influence of the soil structure interaction. The first technique uses the transfer function between the roof and the basement in both directions. The second technique uses a pre-whitening filter on the data obtained from both the basement and the roof. Subsequently the impulse response function is computed from the scaled cross correlation between the input and the output. The overall results showed that the structure will satisfy the life safety performance level in a future earthquake but some soil structure interaction effects should be expected in the North South direction.

**Keywords:** structural health monitoring; reinforced concrete buildings

---

## 1. Introduction

The 1999 Kocaeli and the Duzce earthquakes were milestones in the public awareness regarding the extreme vulnerability of Istanbul to earthquakes. Research reveals that the seismic threat today is even higher for the megacity of Istanbul (Stein *et al.* 2000). The Kocaeli and the Duzce earthquakes in 1999 had claimed the lives of 18,000 people and it was the last of a series of earthquakes that started in 1939 in eastern Turkey and gradually migrated to the west along the

---

\*Corresponding author, Professor, E-mail: [gundesbakir@yahoo.com](mailto:gundesbakir@yahoo.com)

border between the Anatolian and the Eurasian Plates. Subsequently, the next earthquake is expected to hit the Metropolitan city of Istanbul in the west of Kocaeli. Many mitigation activities have been carried out both by the local and the central governments until today. The most important of these studies include the microzonation of Istanbul, preparation of the earthquake Master Plan of the Megacity for the Metropolitan City Municipality and the walk down damage evaluations for the existing buildings by street surveys (Istanbul Metropolitan City Municipality 2010). In spite of its substantial importance, no step towards a systematic instrumentation of the bridges and viaducts on the main arteries of the transportation system or on typical public buildings in Istanbul have been undertaken until today. For a Megacity like Istanbul however, this would be extremely important as vibration monitoring provides many advantages. In the last 10 years or so, there has been significant progress on damage detection by finite element model updating on bridges and buildings. In the finite element model updating technique, the difference between the modal parameters obtained from the vibration monitoring of structures and the modal parameters obtained from the finite element model of the structure are minimized iteratively within an optimization scheme. In each iteration, the finite element model of the structure is updated. The procedure is stopped when the modal parameters obtained from the finite element model are tuned to the experimental data. It has been proven that by using this technique, it is possible to identify the existence, location and the extent of damage in structures (Bakir *et al.* 2007a, 2008). However, up until now, the finite element model updating technique has been applied on data obtained from the periodic monitoring. With the recent advances on electronics of the structural health monitoring systems, it is now possible to monitor and identify structures continuously in real time. This gives hope that we are also very close to identify the existence, location and the extent of damage in structures in real-time using the finite element model updating technique and continuous data. By continuous monitoring, it will also be possible to determine the performance level of buildings immediately after earthquakes and close a building or bridge to operation if a problem exists.

Research on vibration monitoring of bridges have been documented by Bayraktar *et al.* (2009a, b, 2010), Ko *et al.* (2009), Chen *et al.* (2010), Bakir (2011), Tezcan *et al.* (1975), Brownjohn *et al.* (1987, 1992), Fraser *et al.* (2010), Magalhaes *et al.* (2008, 2009), Magalhaes and Cunha (2011) and in buildings by Safak (1993), Kohler *et al.* (2005), Yoshimoto *et al.* (2005), Ventura *et al.* (2003), Hong *et al.* (2009), Bakir *et al.* (2007a, 2008).

In structural health monitoring, structures can be monitored either periodically (i.e., visiting the structure and taking measurements periodically before and after earthquakes) or they can be monitored continuously where the sensors and the data acquisition system are deployed permanently on the structure. In 2008, a TUBITAK (Turkish Scientific and Technological Research Agency) project has been started by the author (Bakir 2008) for monitoring a typical school building in Istanbul, Turkey continuously. The structure is fully instrumented with 17 sensors. This is one of the first large scale instrumentations in Turkey. In previous applications in the country, only a strong-motion accelerograph was deployed in the basement of the public buildings. The aim in those projects was to investigate the seismic activity around the instrumented site rather than structural health monitoring or damage identification in the building. The methodology and the know how acquired from this project will also be extended to other mid rise stiff residential and public buildings in Turkey. The aims of this paper are to test the applicability of subspace based system identification techniques on typical school buildings in Turkey, predict the earthquake performance of these buildings by structural health monitoring and identify the soil structure interaction effects from ambient vibration records.

This study is organized as follows: In the second section, the building site is described first. Within this context, the documentation of the laboratory tests on material and cores taken from the building as well as the site investigations are given. In section 3, results of the analysis from the finite element (FE) modeling and the modal analysis by Block Lanczos method with a sparse matrix solver as well as the performance based evaluation of the building according to the 2007 Turkish Earthquake Resistant Design Code (TERDC) (Ministry of Public Works and Settlement 2007) by both pushover analysis and the nonlinear dynamic time history analysis are given. In section 4, steps in instrumentation (such as cabling, mounting the sensors, etc.) are explained in detail. Section 5 describes the system identification using the Stochastic Subspace based System Identification Technique. Section 6 presents two methodologies for the detection of soil structure interaction effects in buildings from vibration recordings. In section 7, a technique to check the validity of the proportional damping assumption is given. Section 8 summarizes the conclusions.

## 2. Description of the building site

The instrumented school building is located in the Kadikoy district of the Asian part of Istanbul in the Northwestern part of the Marmara region of Turkey as shown in Fig. 1. The building is constructed according to the standard school projects which are used by the Ministry of Education of Turkey until the catastrophic Kocaeli and Duzce earthquakes in 1999. It is a five storey structure with one basement as shown in Fig. 2. The floor system is flat slab with beams. The building has a typical storey height of 3.2 m and is considered as regular in elevation. The dimensions of the beams and the columns are typically  $0.3 \text{ m} \times 0.60 \text{ m}$ .

Cylinder concrete test cores are taken from the building in addition to the 350 Schmidt tests carried out on different columns and the shear walls of the building. As a result, the concrete strength is determined as 27 MPa. In order to determine the site effects, a 20 m deep borehole is drilled. According to the samples taken throughout the borehole, the bedrock starts 4.6 m from the surface which coincides with the foundation of the structure. The site has no liquefaction potential



Fig. 1 Location of the instrumented building



Fig. 2 The instrumented school building (website of the school building)

and geologically, is located in the Kartal formation which is composed of slate and shale. According to the borehole log, the first 2.5 m of the filled soil is composed of materials from the grain size of clay to gravel. From 2.5 m to 4.6 m from the surface, the site is completely segregated slate. From 4.60 m to 20 m, the bedrock is situated which is composed of dark grey, unsegregated slate with or without minimal cracks. The ground water table is at 7.8 m below the surface. A two profile seismic refraction test is carried out. The predominant period of the site is estimated to be between 0.19-0.26 s. As a result of the investigations, the building site is classified as Z2.

### 3 Building numerical models and computer analysis

A three dimensional FE model is built for the analysis based on the blueprints of the school building using the systems analysis software ANSYS (2010). In the first stage, in order to obtain the natural frequencies and the mode shapes of the system, modal analysis is carried out by using the Block Lanczos extraction method with a sparse matrix solver. The first two mode shapes of the frame resulting from the FE model of the structure are shown in Figs. 3 and 4 (Bakir 2011b).

The corresponding modal frequencies are given in Table 1.

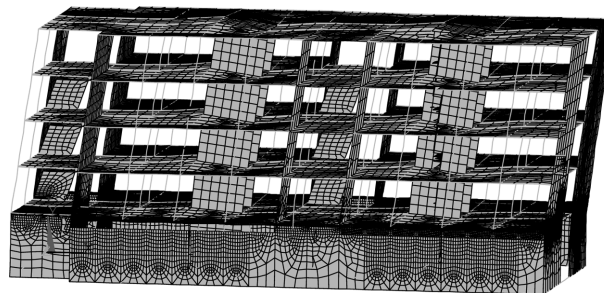


Fig. 3 The first vibration mode (the first bending mode in the long direction)

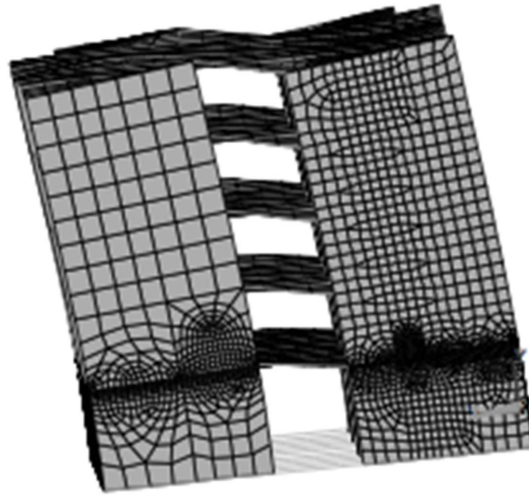


Fig. 4 The second vibration mode (the first bending mode in the short direction)

Table 1 Modal frequencies calculated using the FE model

Number	Frequency (Hz)	Mode type
1	2.62	First bending mode in the z direction
2	4.84	First bending mode in the x direction
3	5.90	First torsion mode
4	10.01	Second bending mode in the z direction
5-12	10.13	Local moeds of the ground storey beams
13	14.26	Local moed of the slabs
14	14.29	Local moed of the slabs
15	14.32	Local moed of the slabs
16	14.60	Local moed of the slabs
17	15.69	Local moed of the slabs
18	15.75	Local moed of the slabs
19	15.87	Local moed of the slabs
20	15.95	Local moed of the slabs

The TERDC has adopted a performance based evaluation strategy for the existing buildings in Turkey. According to the Turkish Code, school buildings have to satisfy the Immediate Occupancy Performance Level for earthquakes with a 10% probability of exceedance within 50 years, also termed the Design Earthquake and the Life Safety Performance Level for earthquakes with a 2% probability of exceedance within 50 years, also termed the Maximum Considered Earthquake (MCE) ground shaking. The performance level of the school building is determined elsewhere (Sezgin 2008, Karakan 2009). Both references confirm that the structure will satisfy the Life Safety Performance Level for the MCE. In the first thesis based on the nonlinear static pushover analysis, it is shown that the building satisfies the Immediate Occupancy Performance Level in the short direction for the design earthquake but not in the long direction. However, in the second thesis in which the nonlinear dynamic time history analysis is used, the building does not satisfy the Immediate Occupancy Performance Level in both the short and the long directions for earthquakes

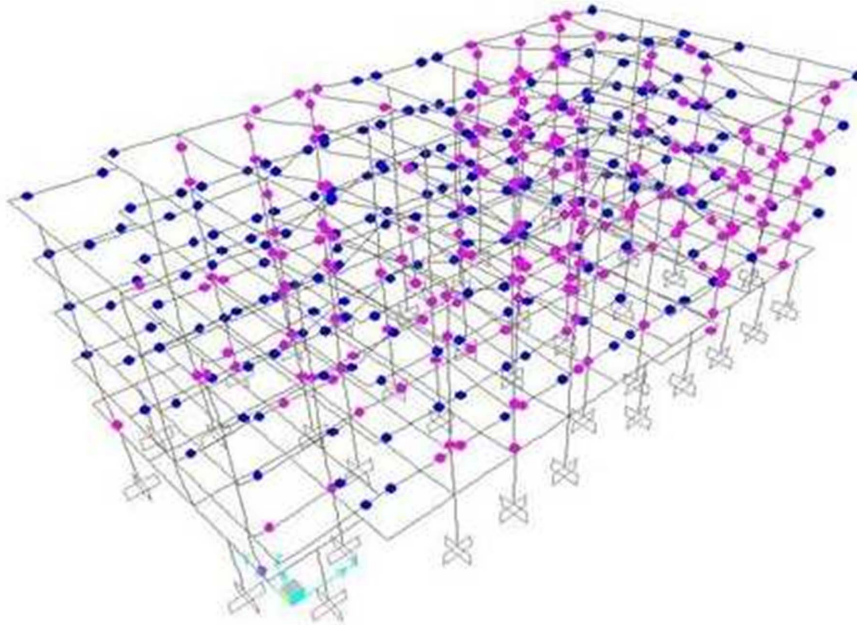


Fig. 5 Plastic hinges that occur in the long direction of the structure due to the Erzincan earthquake: Minimum Damage Level (magenta), and the Moderate Damage Level (blue)

that have 10% probability of exceedance within 50 years. In the second thesis, a nonlinear dynamic time history analysis is applied under 3 different earthquake ground motions, namely 2 records from the Imperial Valley, El-Centro Earthquake of  $M_w = 6.53$  in 1979 and the Erzincan earthquake of  $M_w = 6.69$  in 1992 in Turkey. It is apparent that the worst results are obtained from the Erzincan earthquake. The plastic hinge locations in the building for the long and the short directions are shown in Fig. 5. It is apparent from the results of this analysis that no columns exceed the Minimum Damage Level prescribed by the Turkish Earthquake Resistant Design Code. However, more than 10% of the beams exceed the Minimum Damage Level and are in the Moderate Damage Level. Consequently, the structure satisfies the Life Safety Performance Level but not the Immediate Occupancy Level for the Design Earthquake.

#### 4. Steps in instrumentation

The structural health monitoring system has 14 Kinematics EpiSensor Force Balance Accelerometers (Model FBA ES-U2) in addition to 1 triaxial force balance accelerometer (Model FBA ES-T). The output type of the sensors is differential with a 10 V/g sensitivity. The sensors have full-scale recording range of 2 g and the sensor output voltage level is 10 Volts. The data acquisition system is 24 channel Kinematics Granite.

The first step in the instrumentation is the optimum location of sensors. For this purpose, the author has developed a MATLAB based toolbox OPTISEP (OPTImal Sensor Placement) which can compute the optimum sensor locations according to six alternative optimal sensor placement

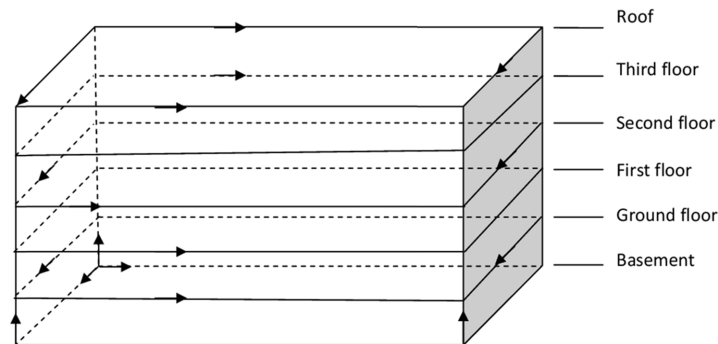


Fig. 6 The sensor configuration obtained from the sensor set expansion technique

techniques currently used in NASA for large space structures. Different techniques that are incorporated in the toolbox are the Effective Independence Method (EFI) developed by Kammer (1991), Optimal Driving Point (ODP) based method (Marek *et al.* 1994, Imamovic 1998, Doebling 1996), Non-Optimal Driving Point (NODP) based method (Imamovic 1998), Effective Independence Driving Point Residue Method, the Singular Value Decomposition based method developed by Kim and Park (1997) and the Sensor Set Expansion Technique developed by Kammer *et al.* (2005). The techniques are compared using the determinant, the trace and the condition number of the Fisher Information Matrix. The results show that the best results are obtained by the Sensor Set Expansion Technique (Bakir 2011c). The resulting sensor configuration is shown in Fig. 6.

Subsequently, the location of the data acquisition system is selected and the cable route drawings that show the cabling system from sensors to the data acquisition system are prepared for each storey. The total cable length is calculated accordingly. The 500 m of cable conduit is mounted by electricians. The 500 m Belden cable is then pulled and routed inside this conduit from sensors to the data acquisition system throughout the structure. The data acquisition system has an internal GPS. The GPS antenna for the data acquisition system is mounted on an iron rod constructed on the roof specially for this purpose. The GPS antenna comes with 25 m of ultraviolet light resistant cable, which can also stay outside the building. The purpose of the GPS antenna in installations is



Fig. 7 The sensor installation

the time synchronization of the system. Next, all the locations and the corresponding directions of the sensors are marked as shown in Fig. 7.

The sensors are installed first in their appropriate positions computed according to the Sensor Set Expansion Technique. The most important rule in this installation is that the sensor edges should be as orthogonal as possible to the two walls of the structure. Since the structure is aligned in the East-West direction, the long side is parallel to the East-West direction and the short side is parallel to the North-South direction. If the sensor is installed with an angle to the sides of the columns or walls, then the recorded data will have to be orthogonally transformed again. In order to avoid this, full care is given to obtain a configuration that is as orthogonal as possible. Soldering of the sensors and the connectors is carried out next. The sensors are leveled and connected to the correct power. The sensors in the basement storey are installed on the floor. In order to obtain a smooth foundation for the sensors, the floor tiles on the ground are first stripped and a flat surface is obtained. Cement grout is poured on this stripped surface. Then the sensors are installed. For these types of sensors on the ground, metal bottomless security boxes with lids are constructed. The data acquisition system is installed in the control room. The DC offset for each accelerometer is measured next. This DC offset has to be as close as possible to zero in order to obtain a record with minimal offset. If there is DC offset in an accelerometer, then a zero adjustment should be performed before the data recording. This is also the case for our system. A static IP address is obtained solely for the data acquisition system along with NetMask, Gateway and DNS (primary or secondary) numbers. By this way, continuous remote monitoring of the school building could become possible. The data acquisition system collects data of 200 samples per second for each sensor from the school building.

## 5. System identification

The modal parameters of the structure are computed using the Stochastic Subspace System Identification Technique (SSI), specifically, the sto-alt algorithm in Van Overschee and De Moor (1996). This technique computes the state space models only from the output data as described in the following subsections.

### 5.1 Data structure

Block Hankel matrices play an important role in the Stochastic SSI. They can be constructed from the input and output data as follows

$$U_{0|2i-1} = \begin{pmatrix} u_0 & u_1 & \dots & u_{j-1} \\ u_1 & u_2 & \dots & u_j \\ \dots & \dots & \dots & \dots \\ u_{i-1} & u_i & \dots & u_{i+j-2} \\ u_i & u_{i+1} & \dots & u_{i+j-1} \\ u_{i+1} & u_{i+2} & \dots & u_{i+j} \\ \dots & \dots & \dots & \dots \\ u_{2i-1} & u_{2i} & \dots & u_{2i+j-2} \end{pmatrix} \dots = \begin{pmatrix} U_{0|i-1} \\ U_{0|2i-1} \end{pmatrix} = \begin{pmatrix} U_p \\ U_f \end{pmatrix} \quad (1)$$

where the subscripts of  $U$  represent the first and the last element of the first column;  $U_{0|i-1}$  is denoted by  $U_p$  and  $U_{i|2i-1}$  by  $U_f$ , the subscripts  $p$  and  $f$  denote the past and the future, respectively,  $i$  is the number of block rows,  $j$  is the number of columns of the block Hankel matrices. From a statistical point of view  $j$  should be much larger than  $i$ . To ensure that all the samples are used,  $j$  is taken as equal to  $s - 2i + 1$ , where  $s$  is the number of samples of the measurement.

The output block Hankel matrices  $Y_{0|2i-1}$ ,  $Y_p$ ,  $Y_f$ , are defined similar to Eq. (1). A block Hankel matrix  $W_{0|i-1}$ , consisting of inputs and outputs can be defined as

$$W_{0|i-1} = \begin{pmatrix} U_{0|i-1} \\ Y_{0|i-1} \end{pmatrix} = \begin{pmatrix} U_p \\ Y_p \end{pmatrix} = W_p \quad (2)$$

## 5.2 Stochastic subspace system identification

The stochastic model that will be identified is given by Van Overschee and De Moor (1996)

$$x_{k+1} = Ax_k + w_k \quad (3)$$

$$y_k = Cx_k + v_k \quad (4)$$

with

$$\mathbf{E} \begin{bmatrix} \begin{pmatrix} w_k \\ v_k \end{pmatrix} \\ (w_l^T \ v_l^T) \end{bmatrix} = \begin{pmatrix} Q & S \\ (S)^T & R \end{pmatrix} \delta_{kl} \quad (5)$$

where  $A, Q \in \mathbb{R}^{n \times n}$ ,  $C \in \mathbb{R}^{l \times n}$ ,  $S \in \mathbb{R}^{n \times l}$  and  $R \in \mathbb{R}^{l \times l}$ . The vectors  $v_k \in \mathbb{R}^{l \times 1}$  and  $w_k \in \mathbb{R}^{n \times 1}$  are unmeasurable, Gaussian distributed zero mean white noise vector sequences,  $l$  is the number of outputs and  $A, C$  are the system matrices of the state space model. Stochastic SSI starts with the calculation of the orthogonal projection of the output data as follows

$$O_i = Y_f / Y_p \quad (6)$$

Subsequently, the singular value decomposition of the weighted projection is calculated as

$$W_1 O_i W_2 = USV^T \quad (7)$$

where  $U = (U_1 \ U_2)$  and  $V = (V_1 \ V_2)$  are the orthonormal matrices (not to be confused with the notation  $U$  used for the input block Hankel matrices) and  $S$  is a diagonal matrix that contains the singular values in the diagonal. In the third step, the extended observability matrix  $\Gamma_i$  takes the following form

$$\Gamma_i = W_1^{-1} U_1 S_1^{1/2} \quad (8)$$

Hence, the state space system matrix  $A$  is computed as

$$A = \underline{\Gamma}_i^\dagger \bar{\Gamma}_i \quad (9)$$

The state-space matrix  $C$  is calculated as the first  $l$  rows of  $\Gamma_i$ .

### 5.3 Determining the modal parameters from the system matrices

The system matrix  $A$  can be decomposed as

$$A = \psi \Lambda_d \psi^{-1} \quad (10)$$

where  $\psi \in C^{n \times n}$  is the eigenvector matrix and  $\Lambda_d \in C^{n \times n}$  is a diagonal matrix that contains the discrete time eigenvalues  $\mu_i$ . The eigenfrequencies are calculated from

$$\lambda_i = \frac{\ln(\mu_i)}{\Delta t} \quad (11)$$

where  $\lambda_i$  denotes the continuous time eigenvalues and  $\Delta t$  is the sampling time. The damping ratio (in %) is computed from

$$\xi_i = -100 \frac{\lambda_i^R}{|\lambda_i|} \quad (12)$$

where  $|\cdot|$  denotes the complex modulus and  $\lambda_i$  is expressed as

$$\lambda_i = \lambda_i^R + i \lambda_i^I \quad (13)$$

The mode shapes  $V$  are computed from

$$V = C \psi \quad (14)$$

### 5.4 System identification

The data obtained from the sensor configuration given in Fig. 6 is decimated with a factor of 2 and then band-pass filtered between 0.05 Hz and 80% of the Nyquist frequency before feeding the data into the Stochastic SSI. Identification is carried out for all orders between 20 to 200 and the results are recorded. One common problem that an expert engineer faces in system identification is the incorrect choice of the model order and problems associated with the discrimination of the physical poles from the spurious ones. If the modal order is specified higher than it actually is, spurious poles will appear in the model. The presence of the noise in the measurements also produces spurious numerical poles. Analog or digital filtering of the data is also known to be a source of the spurious poles in the model.

The tool used for discriminating numerical poles from the physical poles is the stabilization diagram. The stabilization diagram shows the poles of a system at different model orders. The frequency is plotted on the abscis and the model order is plotted on the ordinate of a stabilization diagram. The poles that correspond to an order are compared with the poles of one order lower system.

Physical poles occur at the same frequency at increasing model orders forming a vertical column of poles. In other words, they tend to stabilize, hence the term “stabilization diagram”. An expert engineer then chooses an unknown number of poles at different frequencies. In stabilization diagrams, the stability limits are selected by the user such that

$$\frac{f^n - f^{n+1}}{f^n} < \lim_f \% \quad (15)$$

$$\frac{\xi^n - \xi^{n+1}}{\xi^n} < \lim_\xi \% \quad (16)$$

$$(1 - MAC(n, n+1)) < \lim_{MAC} \% \quad (17)$$

where  $n$  denotes the model order,  $f$  is the frequency,  $\xi$  is the damping ratio,  $\lim_f\%$  is the frequency limit specified by the user,  $\lim_\xi\%$  is the limit for the damping ratio specified by the user,  $\lim_{MAC}\%$  is the limit for MAC -the Modal Assurance Criterion-which can be defined as

$$MAC(n, n+1) = \frac{|\phi^{(n)H} \phi^{(n+1)}|^2}{(\phi^{(n)H} \phi^{(n)})(\phi^{(n+1)H} \phi^{(n+1)})} \quad (18)$$

where  $\phi$  are the identified mode shapes and  $(.)^H$  denotes the complex conjugate transpose (Bakir 2011a). The stabilization diagram obtained from this study is shown in Fig. 8. The stabilization criteria is 1% for the frequencies, 5% for the damping ratios and 1% for the mode shapes. The data is also filtered such that poles with damping ratios less than 0 and higher than 10% are also disregarded. A pole stable in frequency is called an “ $f$ ” type pole, a pole stable in damping and frequency is referred to as a “ $d$ ” type pole, a pole stable in eigenvector and frequency is called a “ $v$ ” type pole and a pole that satisfies all the stability criteria is denoted as an “ $s$ ” type pole.

The frequencies, the damping ratios and the mode shapes identified from this building are shown in Figs. 9-10. It is apparent that the school building is a very stiff structure due to a large number of walls in both directions.

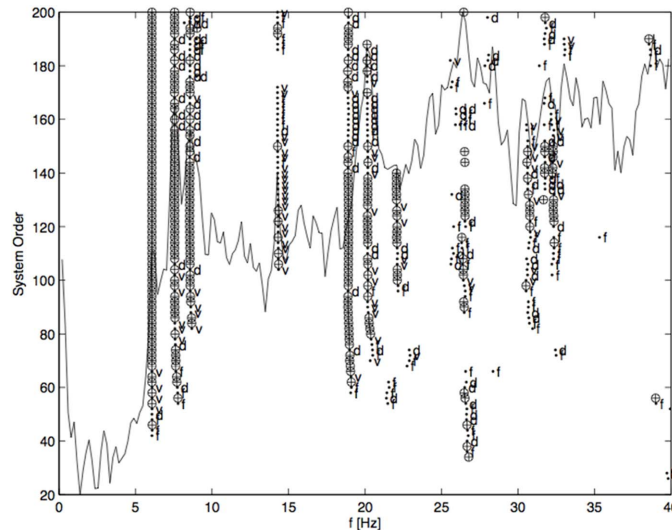


Fig. 8 Stabilization diagram obtained by applying the Stochastic Subspace System Identification Technique to band pass filtered and resampled data

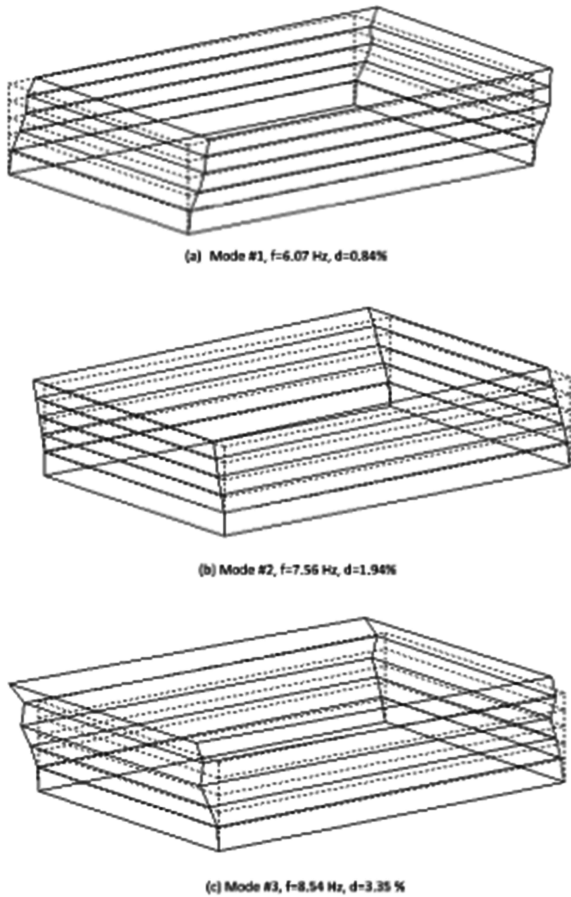


Fig. 9 Frequencies, mode shapes and the damping ratios obtained from system identification for the first 3 modes

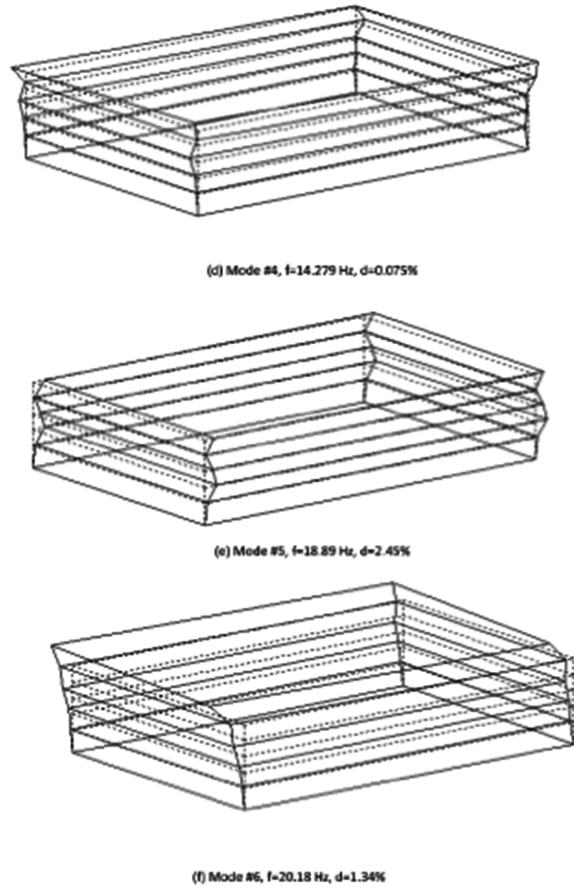


Fig. 10 Frequencies, mode shapes and the damping ratios obtained from system identification for the 4th, 5th and the 6th modes

## 6. Detection of soil structure interaction in buildings from vibration recordings

Soil structure interaction effects substantially affect the modal parameters obtained from the system identification of the vibration data. Since the modal parameters are also affected from damage, it is imperative to determine the extent to which these modal parameters are affected from the soil structure interaction in order to discriminate the changes due to damage. For this reason, the following methodology has been pursued to investigate the presence of soil structure interaction effects in the vibration data: When, the motion of the building does not affect the motion of the free field and the foundation of the building, the building can be assumed to be fixed at the supports. In this case, the vibration recordings at the foundation level can be accepted as the base excitation, i.e., the input to the system. The data obtained from sensors at the different stories of the building are then the output. This is a typical open loop or causal system. Causal because the input at time  $t_i$  can only affect the output at times  $t > t_i$ . However in cases, where the motion of the foundation and the free field are affected from the motion of the superstructure, the system becomes a closed loop

system, i.e., an acausal system where the impulse response function is acausal (Akaike 1967). In this case, there are soil structure interaction effects and the input and the output are coupled. If there is no borehole instrumentation available, it becomes a challenge to determine the extent of these effects. Safak (1995) states that for causal systems, the impulse response of the system is zero for  $t < 0$ ; for acausal systems however, it is not. The author investigates the impulse response of the building from the vibration recordings of the foundation and upper stories. If the impulse response gives significant amplitudes at negative times in comparison to the positive times, there is soil structure interaction. In order to understand whether there are soil structure interaction effects, the impulse response functions are computed by taking the foundation accelerations as the input and the top story accelerations as the output. Both the input  $u$  and the output  $y$  are filtered so that the data are as white as possible. Then the correlation function for these filtered data are calculated as

$$R(\tau) = \frac{1}{N} \sum_{t=\tau}^N y(t)u(t-\tau) \quad (19)$$

The scaled cross correlation function gives the impulse estimate. When there is soil structure interaction, the impulse estimate has amplitudes for  $t < 0$  which have comparable amplitudes to the amplitudes at  $t > 0$ . If there is no soil structure interaction, then the amplitudes when  $t < 0$  are substantially smaller than the amplitudes when  $t > 0$ . Figs. 11 and 12 show the impulse estimates obtained from the top storey and the foundation accelerations in the North South (NS) and East West (EW) directions, respectively. It is apparent that the impulse amplitudes for positive and negative lags are comparable for both the NS and the EW directions under ambient vibrations. Safak has recommended this technique for identifying the soil structure interaction for both ambient as well as strong ground motion excitations (Safak 2010). The figures indicate that there are some sort of soil structure interaction effects in this site although the borehole drills and laboratory tests

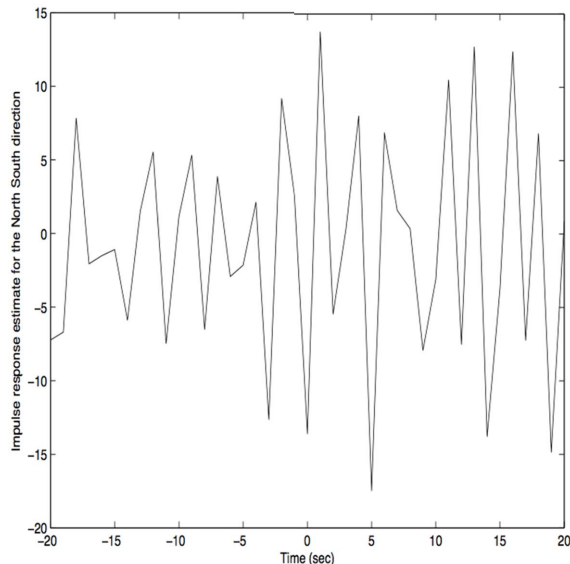


Fig. 11 Impulse response function in the NS direction (shorter direction) obtained from the top storey and foundation accelerations

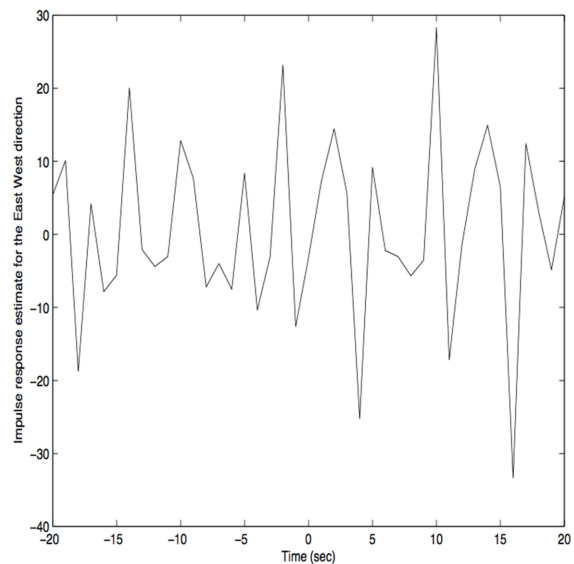


Fig. 12 Impulse response function in the EW direction (longer direction) obtained from the top storey and foundation acceleration

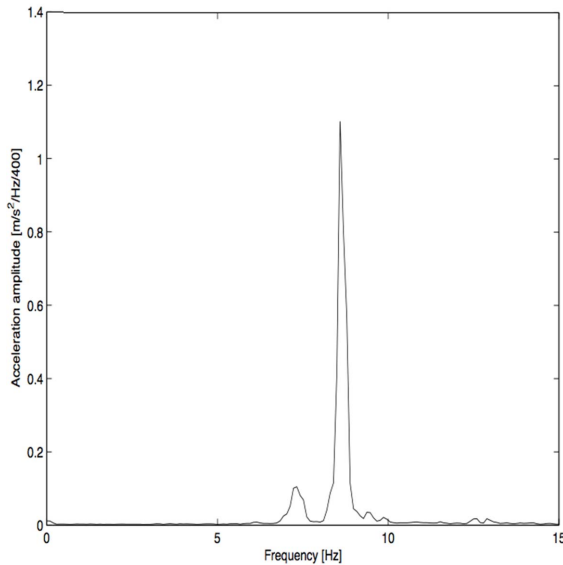


Fig. 13 Ratio of the Fourier amplitude spectra of the top storey to the basement in the NS direction (divided by 400)

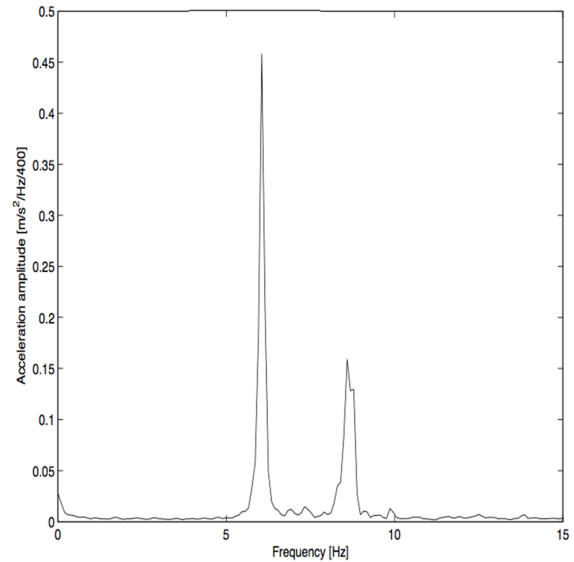


Fig. 14 Ratio of the Fourier amplitude spectra of the top storey to the basement in the EW direction (divided by 400)

as well as the SPT tests have shown that the ground can be classified as rock.

Subsequently, the ratio of the Fourier transforms of the top story and the basement accelerations are computed for both orthogonal directions. The dominant peak in this plot gives the fundamental frequency of the building with fixed base. If this frequency is different than the frequency identified with the stochastic subspace based system identification, then there is soil structure interaction in the system.

The transfer functions in the NS and the EW directions are given in Figs. 13 and 14. In the EW direction, the two frequencies coincide showing that no real soil structure interaction effect is present in the EW direction. The frequency that corresponds to the dominant peak in the transfer function plot for the NS direction is 8.594 Hz. This is the frequency of the building with fixed base. This mode shape is bending in the short direction and identification results showed that the resonance frequency for this mode is 7.56 Hz. Thus, it is apparent that there are soil structure interaction effects in this direction and the period of the building has elongated from that of the fixed case.

## 7. A simple technique to check the validity of the proportional damping assumption

When the damping matrix becomes diagonal under a modal coordinate transformation where the undamped mode shapes of the system are used as basis vectors, damping in the system is called “proportional damping”. This is often the assumption used in dynamic analysis. The damping ratios are often used to specify a measure of the damping resistance associated with the internal friction since it is rather difficult otherwise to relate the damping mechanism to measurable physical

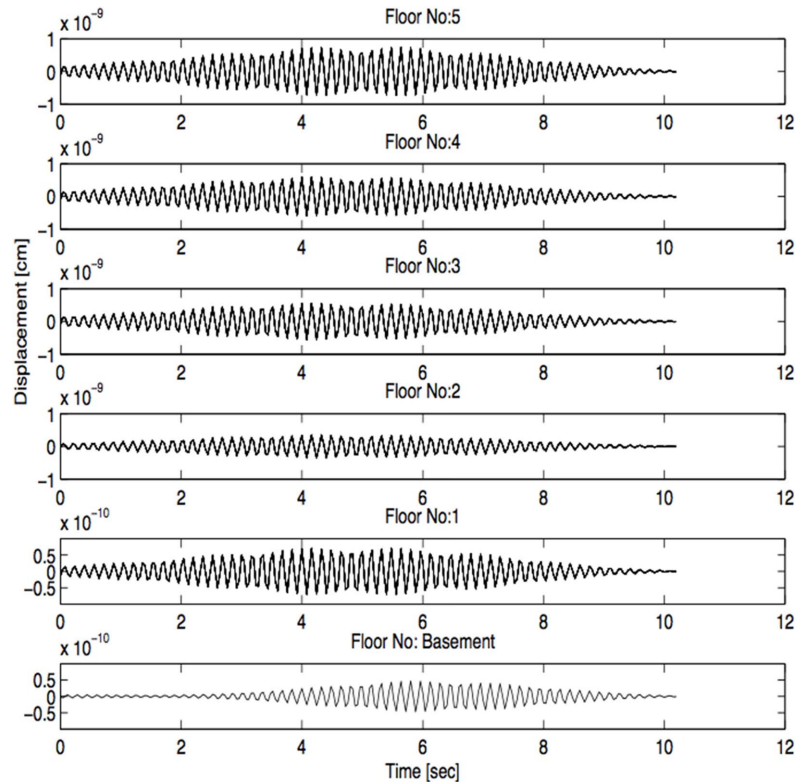


Fig. 15 Displacements in the  $x$  direction (First mode)

characteristics. There are three physical characteristics of damping. First, in flexible structures such as high rise buildings, it is rather difficult to expect the “proportional damping assumption” to hold strictly. In this case, we expect typically “non proportional damping” where the mode shapes are complex. For structures in which the proportional damping assumption holds on the other hand, we expect the mode shapes to be real. Second, in flexible structures, the damping ratios are expected to be lower compared to stocky and stiff buildings. Third, as the mode number increases, we expect the damping ratio also to increase. Since the structure investigated for this case is a stiff reinforced concrete building, the proportional damping assumption is expected to be valid. To check the validity of this assumption, a simple technique is employed. First, the data from all stories are mean removed, averaged, baseline corrected, decimated and band pass filtered where the center frequency is the resonant frequency for the associated mode. Then data from each story is double integrated and the displacements are obtained. If the peaks from each story coincide and there are no phase differences, then the “proportional damping assumption” is valid. Otherwise, some form of “non-proportional damping” should be expected. The displacements in the  $x$  direction are given in Fig. 15. The results show that the “proportional damping” assumption is valid for this building for the first mode. Although not shown here for purposes of brevity, the same analysis is also repeated for other modes and no phase differences are observed.

## 8. Conclusions

Turkey is situated in a substantially seismically active area where earthquakes result in significant loss of life and property. It is also known that a catastrophic earthquake is expected within the next 20 years in Istanbul. This study is a modest attempt to contribute to the mitigation of earthquake hazard in Istanbul. For this purpose, a typical school building in Istanbul is instrumented with 17 accelerometers and is continuously monitored. The aim is forecasting the damage that will occur in typical school buildings due to the expected catastrophic Istanbul earthquake and facilitate fast and accurate risk management. Supplementary to the monitoring, a series of other structural analysis and material tests are carried out.

The results of the above mentioned tests and analysis together with the continuous monitoring of the structure suggest the following significant points about the health of the building: First, the performance based evaluation of the existing structure by both pushover analysis and the nonlinear dynamic time history analysis showed that the structure satisfies the Life Safety Performance Level under a Maximum Considered Earthquake in both directions. Nonlinear dynamic time history analysis on the building has shown that under a Design Earthquake, the structure does not satisfy the Immediate Occupancy Performance Level in both directions. However, it is apparent that this is mainly due to the fact that more than 10% of the beams reach the Moderate Damage Level. The columns of the structure on the other hand do not exceed the Minimum Damage Level imposed by the TERDC. A detailed FE model of the structure is prepared that includes the slabs, the stairs, the columns, the shear walls and the beams. Modal analysis of the structure using the Block Lanczos extraction method with a sparse matrix solver shows that the structure is very stiff and only the first four global modes can be identified using a detailed FE model, namely the first bending in the long direction, the first bending in the short direction, the torsional mode and the second bending in the long direction. From the fifth mode onwards, local modes start which are not of interest for the

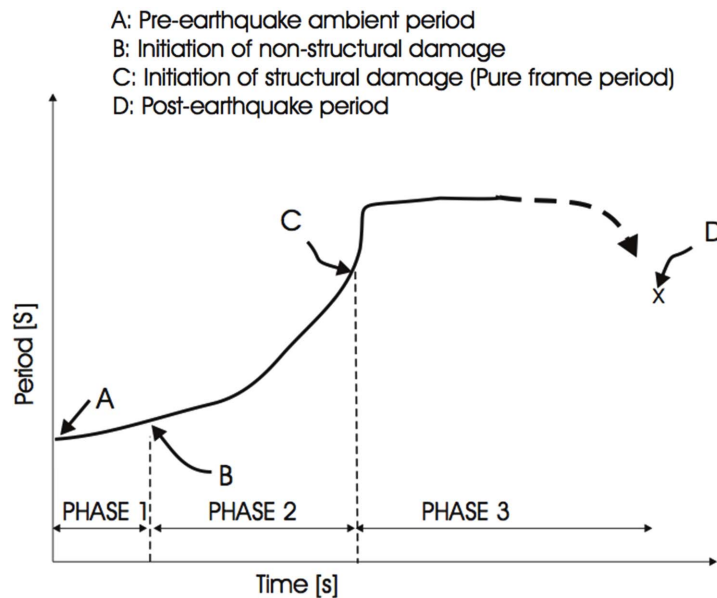


Fig. 16 Variation of the periods during the duration of the earthquakes

seismic safety of the structure. The continuous monitoring of the structure and the system identification at first sight reveal that the structure is even considerably stiffer than what is predicted by the FE model. This controversy will always be observed in the continuous monitoring of the very stiff or stocky structures such as this one. The main reason behind this dilemma is the following: Since the building is used for schooling purposes, it has a large number of partition walls which contribute substantially to the lateral stiffness of the building as long as they are not cracked. Under ambient vibrations, their beneficiary effect is expected to reach a peak. However, under strong earthquakes, it is not appropriate to rely on the lateral stiffness of these partitioning walls, which will inevitably crack. Consequently, the frequencies will be controlled by the bare frame alone. This period elongation confirms the findings in a previous paper of the author (Bakir *et al.* 2007b) and is reshown in Fig. 16 again due to its immense importance.

Transfer functions in both directions showed that soil structure interaction effects may be prevalent in the NS direction in a future earthquake. On the other hand, no SSI effects are observed for the EW direction. This study shows that the vibration monitoring of structures should always be supplemented by the conventional numerical structural analysis techniques due to the fact that the dynamic behavior of structures under ambient vibrations can be different from the dynamic behavior of structures under strong earthquakes. However, in the long term, ambient vibration monitoring would always be critically useful to detect any changes in the health of the structure over time and would facilitate a comparison between the modal parameters of structures before and after catastrophic earthquakes.

This study also gives a detailed review of the steps and the results of the monitoring of a stiff and stocky reinforced concrete building to researchers. It is apparent that the frequencies obtained from the system identification will not match with that obtained from the FE analysis, as under ambient vibrations, the partitioning walls contribute substantially to the lateral stiffness of the building. However, in a large earthquake, it will not be safe to rely on this resistance as once the partitioning walls crack, the bare frame will contribute to the lateral stiffness of the building alone. Consequently, the periods obtained from the system identification will approach those obtained from the FE analysis. The existence of soil structure interaction are also investigated. The results show that the soil structure interaction effects should be expected at least in the NS direction for this building. The results of the full check up in the building shows that the school building is considerably safe as of March 2010 and will endure the expected Istanbul earthquake with minimal or no structural damage and without any loss of life.

## Acknowledgments

This study is carried out in the framework of the TUBITAK project 107M573 for which the author is the promotor. This support is acknowledged here.

## References

- Akaike, H. (1967), "Some problems in the application of the cross spectral method", Spectral Analysis of Time Series, Ed. B. Harris, John Wiley and Sons, NY, USA.
- ANSYS (2010), *Robust Simulation and Analysis Software*, <http://www.ansys.com>, release 10.0, ANSYS

- incorporated.
- Bakir, P.G. (2008), "Damage identification in existing buildings using real time system identification techniques and finite element model updating", In TUBITAK Project No:107M573, ITU, Istanbul, Turkey.
- Bakir, P.G. (2011a), "Automation of the stabilization diagrams for subspace based system identification", *Exp. Syst. Appl.*, **38**(12), 14390-14397.
- Bakir, P.G. (2011b), "Deterministic stochastic subspace system identification in buildings", *Struct. Eng. Mech.*, **38**(2), 315-332.
- Bakir, P.G. (2011c), "Evaluation of optimal sensor placement techniques for parameter identification in buildings", *Math. Comput. Appl.* (in press)
- Bakir, P.G., Reynders, E. and De Roeck, G. (2007a), "Sensitivity based finite element model updating using constrained optimization with a trust region algorithm", *J. Sound Vib.*, **305**(1-2), 211-25.
- Bakir, P.G., De Roeck, G., Degrande, G. and Wong, K.K.F. (2007b), "Seismic risk assessment for the mega-city of Istanbul: Ductility, strength and maximum interstorey drift demands", *Soil Dyn. Earthq. Eng.*, **27**(12), 1101-1117.
- Bakir, P.G., Reynders, E. and De Roeck, G. (2008), "An improved finite element model updating method by the global optimization technique 'Coupled Local Minimizers'", *Comput. Struct.*, **86**(11-12), 1339-1352.
- Bayraktar, A., Altunisik A.C., Sevim, B. and Turket, T. (2009a), "Modal testing, finite element model updating, and dynamic analysis of an arch type steel foot- bridge", *J. Perform. Constr. Facil.*, **23**(3), 81-89.
- Bayraktar, A., Birinci, F. and Altunisik, A.C. (2009b), "Finite element model updating of Senyuva historical arch bridge using ambient vibration tests", *Baltic J. Road Bridge Eng.*, **4**(4), 177-185.
- Bayraktar, A., Altunisik, A.C. and Birinci, F. (2010), "Finite-element analysis and vibration testing of a two-span masonry arch bridge", *J. Perform. Constr. Facil.*, **24**(1), 46-52.
- Brownjohn, J.M.W., Dumanoglu, A.A., Severn, R.T. and Taylor, C.A.L. (1987), "Ambient vibration measurements of the Humber Suspension Bridge and comparison with calculated characteristics", *Proceedings of the ICE*, **83**, 561-600.
- Brownjohn, J.M.W., Dumanoglu, A.A. and Severn, R.T. (1992), "Ambient vibration survey of the Fatih Sultan Mehmet (Second Bosphorus) suspension bridge", *Earthq. Eng. Struct. D.*, **21**, 907-924.
- Chen, B., Xu, Y.L. and Zhao, X. (2010), "Integrated vibration control and health monitoring of building structures: a time-domain approach", *Smart Struct. Syst.*, **6**(7), 811-835.
- Doebling, S.W. (1996), "Measurement of structural flexibility matrices for experiments with incomplete reciprocity", PhD Thesis, Colorado University, <http://sdel.colorado.edu/Publications/1995/Theses/Doebling PhD.pdf>, USA.
- Fraser, M., Elgamal, A., He, X.F. and Conte, J.P. (2010), "Sensor network for structural health monitoring of a highway bridge", *J. Comput. Civil Eng.*, **24**(1), 11-24.
- Gundes Bakir, P. (2011), "The combined deterministic stochastic subspace based system identification in buildings", *Struct. Eng. Mech.*, **38**(3), 315-332.
- Hong, A.L., Betti, R. and Lin, C.C.I. (2009), "Identification of dynamic models of a building structure using multiple earthquake records", *Struct. Control Health. Monit.*, **16**(2), 178-199.
- Imamovic, N. (1998), "Model validation of large finite element model using test data", PhD Thesis, Imperial College, London, UK.
- Kammer, D.C. (2005), "Sensor set expansion for modal vibration testing", *Mech. Syst. Signal Pr.*, **19**(4), 700-716.
- Kammer, D.C. (1991), "Sensor placement for on-orbit modal identification and correlation of large space structures", *J. Guid. Control Dyn.*, **14**(2), 251-259.
- Karakan, P. (2009), "Determining the performance level of an existing reinforced concrete structure using static pushover and dynamic time history analysis", MSc Thesis, Institute of Science and Technology, Istanbul Technical University, Maslak, Istanbul, Turkey.
- Kim, H.B. and Park, Y.S. (1997), "Sensor placement guide for structural joint stiffness model improvement", *Mech. Syst. Signal Pr.*, **11**(5), 651-672.
- Ko, J.M., Ni, Y.Q., Zhou, H.F., Wang, J.Y. and Zhou, X.T. (2009), "Investigation concerning structural health monitoring of an instrumented cable-stayed bridge", *Struct. Infrastr. Eng.*, **5**(6), 497-513.
- Kohler, M.D., Davis, P.M. and Safak, E. (2005), "Earthquake and ambient vibration monitoring of the steel-

- frame UCLA factor building”, *Earthq. Spectra*, **21**(3), 715-736.
- Magalhaes, F. and Cunha, A. (2011), “Explaining operational modal analysis with data from Ana arch bridge”, *Mech. Syst. Signal Pr.*, **25**(5), 1431-1450.
- Magalhaes, F., Cunha, A. and Caetano, E. (2008), “Dynamic monitoring of a long span arch bridge”, *Eng. Struct.*, **30**, 3034-3044.
- Magalhaes, F., Cunha, A. and Caetano, E. (2009), “Online automatic identification of the modal parameters of a long span arch bridge”, *Mech. Syst. Signal Pr.*, **23**(2), 316-329.
- Marek, E.L., Larson, C.B. and Zimmerman, D.C. (1994), “A comparison of modal test planning techniques: excitation and sensor placement using the NASA 8-bay truss”, *Proceedings of the 12th International Modal Analysis Conference*, Honolulu, Hawaii.
- Ministry of Public Works and Settlement (2007), *Specification for Structures to be Built in Disaster Areas*, Government of Republic of Turkey.
- Safak, E. (1993), “Response of a 42 storey steel frame building to the Ms=7.1 Loma-Prieta earthquake”, *Eng. Struct.*, **15**(6), 403-421.
- Safak, E. (1995), “Detection and identification of soil structure interaction in buildings from vibration recordings”, *J. Struct. Eng., ASCE*, **121**(5), 899-906.
- Sezgin, G. (2008), “Determining the performance level of an existing reinforced concrete structure using pushover analysis and according to different soil types”, MSc Thesis, Institute of Science and Technology, Istanbul Technical University, Maslak, Istanbul, Turkey.
- Stein, R.R.S. Barka, A. Parsons, T., Toda, S. and Dieterich, J.H. (2000), “Heightened odds of large earthquakes near Istanbul: An interaction based probability calculation”, *Science*, **288**(5466), 661-665.
- Tezcan, S., Ipek, M., Petrovski, J. and Paskalov, T. (1975), “Forced vibration survey of Istanbul Bogazici Bridge”, *Proceedings of the 5th ECEE*, Vol. 2, Istanbul, Turkey.
- Van Overschee, P. and De Moor, B. (1996), *Subspace Identification for Linear Systems*, Kluwer Academic Publishers, Massachusetts, USA.
- Ventura, C.E., Finn, W.D.L., Lord, J.F. and Fujita, N. (2003), “Dynamic characteristics of a base isolated building from ambient vibration measurements and low level earthquake shaking”, *Soil Dyn. Earthq. Eng.*, **23**(4), 313-22.
- Yoshimoto, R., Mita, A. and Okada, K. (2005), “Damage detection of base- isolated buildings using multi-input multi-output subspace identification”, *Earthq. Eng. Struct. Dyn.*, **34**(3), 307-324.
- Website of the instrumented building (last accessed: 2007), Available at: [www.erenkoy.k12.tr/](http://www.erenkoy.k12.tr/).
- Website of the Istanbul Metropolitan City Municipality (last accessed: 2010), [http : //www.ibb.gov.tr](http://www.ibb.gov.tr).